Geophys. J. Int. (1998) **132,** 181–190

Secular variation of the poloidal magnetic field at the core–mantle boundary

Archana Bhattacharyya
Indian Institute of Geomagnetism, Mumbai, India. E-mail: archana@iigm0.ernet.in

Accepted 1997 August 1. Received 1997 June 25; in original form 1996 May 29

SUMMARY

A region of enhanced conductivity at the base of the mantle is modelled by an infinitesimally thin sheet of uniform effective conductance adjacent to the core–mantle boundary. Currents induced in this sheet by the temporally varying magnetic field produced by the geodynamo give rise to a discontinuity in the horizontal components of the poloidal magnetic field on crossing the sheet, while the radial component is continuous across the sheet. Treating the rest of the mantle as an insulator, the horizontal components of the poloidal magnetic field and their secular variation at the top of the core are determined from geomagnetic field, secular variation and secular acceleration models. It is seen that for an assumed effective conductance of the sheet of 10^8 S, which may be not unrealistic, the changes produced in the horizontal components of the poloidal field at the top of the core are usually ≤ 10 per cent, but corrections to the secular variation in these components at the top of the core are typically 40 per cent, which is greater than the differences that exist between different secular variation models for the same epoch. Given the assumption that all the conductivity of the mantle is concentrated into a thin shell, the present method is not restricted to a weakly conducting mantle. Results obtained are compared with perturbation solutions.

Key words: core–mantle boundary, mantle conductivity, poloidal field, secular variation.

INTRODUCTION

In a number of studies of the fluid flow and flow shear near the top of the core (Barraclough, Gubbins & Kerridge 1989; Lloyd & Gubbins 1990; Jackson & Bloxham 1991), the poloidal magnetic field at the core–mantle boundary (CMB) has been determined by downward continuation of the magnetic field at the surface of the Earth to the CMB using a spherical harmonic representation for the scalar potential everywhere in the mantle, which is assumed to be an insulator. One of the main reasons cited for not correcting the poloidal field at the CMB for a non-zero mantle conductivity is the lack of adequate knowledge of the conductivity of the lower mantle below depths of 2000 km. Electromagnetic induction studies yield reliable mantle conductivity profiles only down to depths of around 1000 km (Parkinson & Hutton 1989), where the conductivity is not appreciable in any case. The other reason for not including a non-zero mantle conductivity in the above studies is based on the results obtained by Benton & Whaler (1983), who developed a perturbation technique to deduce the poloidal field at the CMB by solving the poloidal diffusion equation in a weakly conducting mantle. These authors found that for a range of conductivity profiles for the mantle, the corrections to the radial component of the magnetic field and its secular variation at the CMB are typically 2 and 10 per cent respectively. Given the accuracy of the magnetic field models before MAGSAT, it was felt that corrections of this magnitude were not meaningful.

In the last decade it has emerged that the lowermost reaches of the mantle may have enhanced conductivity. Knittle & Jeanloz (1989, 1991) have suggested that infiltration of core material into this region may be responsible for the high conductivity. Another mechanism, favoured by other workers, is the presence of crypto-continental areas at the base of the mantle (Stacey 1992). This region near the CMB may correspond in part to the seismologically identified D″ layer, which has a thickness of 200–300 km. Poirier & Le Mouël (1992) have looked into the question of what effect the infiltrated core material in the lower mantle might have on the observed geomagnetic field. In order to estimate the upper limit for such an effect, they considered an extreme situation where all the infiltrated iron is segregated into a single spherical mass, which, according to their estimate, would have a radius of about 250 km. Electric currents induced in this spherical inclusion, located close to the CMB, due to the temporally varying magnetic field produced by the geodynamo operating in the outer core, would contribute to the secular variation at the surface of the Earth. Poirier & Le Mouël (1992) estimate this

contribution to be smaller than the secular variation in the source-free mantle case by a factor $(r_i/R)^3 \sim 7 \times 10^{-4}$, where r_i is the radius of the inclusion and R is the distance of the point of observation from the centre of the inclusion. From their arguments it would appear that if, instead of the single spherical inclusion near the CMB, a thin spherical shell of highly conducting material of radius equal to that of the outer core surrounded the core, currents induced in this shell could have an observable effect on the secular variation at the surface of the Earth. It may be not implausible to assume that such a thin layer of high electrical conductivity exists at the CMB. As such, this layer would be expected to have a great deal of lateral variation in conductivity due to the presence of highly conducting patches, which may be identified with crypto-continents (Stacey 1992). In the present paper, a simplified picture is considered wherein a spherical shell of uniform effective conductance and negligible thickness is located adjacent to the CMB while the rest of the mantle is assumed to be an insulator. This approximation is used in the next section to relate the horizontal components of the poloidal field at the top of the core, just beneath this layer, to those immediately above the layer, where the mantle is an insulator and the horizontal components are known. The horizontal components thus derived and their secular variation are discussed in the third section. In the section following that, it is demonstrated that a perturbation approach for solving the diffusion equation for the poloidal field in a thin, highly conducting layer adjacent to the CMB yields results which, to the lowest order in the thickness of the layer, are in agreement with the results of this paper. The paper concludes with a discussion of the effect of such calculations on estimates of the flow shear near the top of the core, and the limitations of the present calculations.

THIN CONDUCTING SHEET AT THE CMB

Experiments at high pressures and temperatures (Knittle & Jeanloz 1989, 1991) have indicated that it is possible that some of the highly conducting core material infiltrates into the lower mantle to form a thin layer of conductivity σ as high as 10^3 S m^{-1}. If the average thickness of this layer is around 100 km, the effective conductance could be 10^8 S (Stewart *et al.* 1995). In the stationary conducting layer, neglecting the displacement current, Maxwell's equations require

$$\nabla \cdot \mathbf{B} = 0, \tag{1}$$

$$\nabla \times \mathbf{H} = \mathbf{J}, \tag{2}$$

$$\nabla \times \mathbf{E} = -\frac{\partial \mathbf{B}}{\partial t}. \tag{3}$$

The current density $\mathbf{J}$ and electric field $\mathbf{E}$ are related through Ohm's law:

$$\mathbf{J} = \sigma \mathbf{E}. \tag{4}$$

In certain geophysical problems such as electromagnetic induction of currents in oceans and the ionosphere, the highly conducting region has often been modelled as an infinitesimally thin sheet (Chapman & Whitehead 1923; Lahiri & Price 1939) to make the theory more tractable. It is possible to make this approximation when the thickness of the conducting layer is much smaller than the typical wavelength of a varying magnetic field (Rikitake 1966). With the assumption that all the conductivity of the mantle is concentrated into a thin spherical shell at the base of the mantle, it is possible to study the effect of this shell on secular variations in large-scale ($\gg$100 km) poloidal magnetic fields produced by the geodynamo in the fluid outer core, by replacing this shell by an infinitesimally thin spherical sheet adjacent to the CMB.

A sheet current density $\mathbf{I}_s$ is now defined by integrating the horizontal component $\mathbf{J}_s$ of $\mathbf{J}$ over the thickness δ of the shell at any point:

$$\mathbf{I}_s = \int_c^{c+\delta} \mathbf{J}_s \, dr, \tag{5}$$

where c is the radius of the outer core. The conductance, $\mathscr{G}$, of the sheet is defined by

$$\mathscr{G} = \int_c^{c+\delta} \sigma \, dr. \tag{6}$$

The tangential component $\mathbf{E}_s$ of $\mathbf{E}$, which remains continuous on crossing the sheet, can be written as

$$\mathbf{E}_s = \mathbf{I}_s / \mathscr{G}. \tag{7}$$

Following the theory of electromagnetic induction in a thin conducting sheet (Lahiri & Price 1939; Rikitake 1966), eq. (2) is integrated over an infinitesimal area enclosed by a rectangle with two sides of length δl parallel to the sheet and on opposite sides of it, to obtain, using Stokes' theorem,

$$\hat{\mathbf{r}} \times (\mathbf{H}_m - \mathbf{H}_c) = \mathbf{I}_s, \tag{8}$$

where $\hat{\mathbf{r}}$ is a unit vector normal to the spherical sheet and $\mathbf{H}_m$ and $\mathbf{H}_c$ are respectively the magnetic fields on the mantle and core sides of the sheet. Here $\mathbf{H}_c$ includes a toroidal component as well, due to non-vanishing radial currents at the top of the core, and $\mathbf{I}_s$ also includes contributions from poloidal currents which flow in the core and close their loops in part through the conducting sheet adjacent to the CMB. Integration of the solenoidal condition $\nabla \cdot \mathbf{J} = 0$ over a volume enclosed by a cylindrical box of negligible height spanning the conducting sheet, with its ends parallel to the sheet, yields for the radial component of the current at the top of the core

$$J_{cr} = \nabla_s \cdot \mathbf{I}_s, \tag{9}$$

with ∇_s denoting the horizontal gradient because the contribution to the equivalent surface integral from the sides of the cylinder does not vanish. Hence, eq. (8) does not require that the toroidal field is negligible. Continuity of the radial (normal) component of $\mathbf{B}$ is seen by integrating the solenoidal condition eq. (1). Integration of eq. (3) over an infinitesimal area in the surface of the sheet itself yields

$$(\nabla \times \mathbf{E}_s) \cdot \hat{\mathbf{r}} = -\frac{\partial B_r}{\partial t}. \tag{10}$$

Substitution of eqs (7) and (8) in eq. (10) leads to the following condition on the jump in $\mathbf{H}$ due to the sheet current:

$$\frac{1}{\mathscr{G}} \nabla_s \cdot (\mathbf{H}_m - \mathbf{H}_c) + \nabla_s \left(\frac{1}{\mathscr{G}} \right) \cdot (\mathbf{H}_m - \mathbf{H}_c) = -\frac{\partial B_r}{\partial t}. \tag{11}$$

This equation gives the general relation between the varying total magnetic fields on the two sides of an infinitesimally thin sheet with a distribution of conductivity, irrespective of how these fields are produced. If the spherical sheet is assumed to have uniform conductance then the second term on the left-hand side of eq. (11) drops out. The mantle outside the sheet

is considered to be an insulator so that $\mathbf{B}_m = \mu_0 \mathbf{H}_m$ can be derived from the scalar potential V:

$$\mathbf{B}_m = -\nabla V, \tag{12}$$

$$V = a \sum_{n=1}^{\infty} \sum_{m=0}^{n} [g_n^m(t) \cos m\phi + h_n^m(t) \sin m\phi] \left(\frac{a}{r}\right)^{n+1} P_n^m(\cos\theta), \tag{13}$$

where a is the mean radius of the Earth's surface.

Here it must be pointed out that strong currents induced in the conducting sheet would change the magnetic field in the core as well, and hence the fluid flow. The field $\mathbf{B}_c$ considered here is the resultant field generated at the top of the core by the dynamo operating in the fluid outer core, overlain by a mantle which has a conducting layer at its base adjacent to the CMB. In other words, $\mathbf{B}_c$ could be obtained by solving the dynamo equations with the appropriate boundary condition. Since $\mathbf{B}_c$ is solenoidal, it can be split into toroidal and poloidal parts $\mathbf{B}_T$ and $\mathbf{B}_P$:

$$\mathbf{B}_c = \nabla \times (T\hat{\mathbf{r}}) + \nabla \times \nabla \times (P\hat{\mathbf{r}}), \tag{14}$$

$$\mathbf{B}_T = \left(0, \frac{1}{r \sin\theta} \frac{\partial T}{\partial \phi}, -\frac{1}{r} \frac{\partial T}{\partial \theta}\right), \tag{15}$$

$$\mathbf{B}_P = \left(\frac{\mathbf{L}^2 P}{r^2}, \frac{1}{r} \frac{\partial^2 P}{\partial r \partial \theta}, \frac{1}{r \sin\theta} \frac{\partial^2 P}{\partial r \partial \phi}\right), \tag{16}$$

where the operator $\mathbf{L}^2$ is defined by

$$\mathbf{L}^2 = -\left[\frac{1}{\sin\theta} \frac{\partial}{\partial \theta}\left(\sin\theta \frac{\partial}{\partial \theta}\right) + \frac{1}{\sin^2\theta} \frac{\partial^2}{\partial \phi^2}\right]. \tag{17}$$

The corresponding current density $\mathbf{J}_c$ is given by

$$\mu_0 \mathbf{J}_c = \nabla \times \nabla \times (T\hat{\mathbf{r}}) + \nabla \times [(-\nabla^2 P)\hat{\mathbf{r}}]. \tag{18}$$

As mentioned earlier, T is non-vanishing at the top of the core because $\mathbf{J}_{cr}$ need not vanish at the top of the core in the presence of a conducting sheet at the base of the mantle. However, since $\nabla_s \cdot \mathbf{B}_T = 0$, the toroidal part of the core field does not contribute to eq. (11) when the sheet is assumed to have uniform conductance. Thus, in the presence of an infinitesimally thin, uniformly conducting sheet at the base of the mantle, it is possible to determine only the poloidal scalar P and its radial gradient $\partial P/\partial r$ at the top of the core using condition (11) and the continuity of B_r.

The average $\langle P \rangle$ of P over the surface of a sphere $r =$ constant can be assumed to vanish, without any loss of generality, since the addition of an arbitrary function of r alone to P has no effect on $\mathbf{B}_P$. Thus P can be expanded in terms of surface spherical harmonics as follows:

$$P = \sum_{n=1}^{\infty} \sum_{m=0}^{n} [S_n^{mc}(r, t) \cos m\phi + S_n^{ms}(r, t) \sin m\phi] P_n^m(\cos\theta). \tag{19}$$

According to eqs (12), (13), (16) and (19), continuity of B_r across the conducting sheet at the base of the mantle ($r = c$) implies that

$$S_n^{mc}(c, t) = \frac{a^2}{n} \left(\frac{a}{c}\right)^n g_n^m, \tag{20}$$

$$S_n^{ms}(c, t) = \frac{a^2}{n} \left(\frac{a}{c}\right)^n h_n^m. \tag{21}$$

The solenoidal condition $\nabla \cdot \mathbf{B}_c = 0$ implies that

$$\nabla_s \cdot \mathbf{H}_c = -\frac{1}{\mu_0 r^2} \frac{\partial}{\partial r}(r^2 B_{cr}), \tag{22}$$

where it has to be kept in mind that although $B_{cr} = B_{mr}$ at the CMB, the radial gradient of B_r need not be continuous across the conducting sheet. Hence eqs (16) and (19) must be used to calculate the right-hand side of eq. (22):

$$-\frac{1}{\mu_0 r^2} \frac{\partial}{\partial r}(r^2 B_{cr}) = -\frac{1}{\mu_0} \sum_{n=1}^{\infty} \frac{n(n+1)}{r^2} \sum_{m=0}^{n} \left(\frac{\partial S_n^{mc}}{\partial r} \cos m\phi + \frac{\partial S_n^{ms}}{\partial r} \sin m\phi\right) P_n^m(\cos\theta), \tag{23}$$

whereas $\nabla_s \cdot \mathbf{H}_m$ can be obtained from eqs (12) and (13):

$$\nabla_s \cdot \mathbf{H}_m = \frac{1}{\mu_0} \sum_{n=1}^{\infty} \frac{n(n+1)}{r} \sum_{m=0}^{n} (g_n^m \cos m\phi + h_n^m \sin m\phi) \times \left(\frac{a}{r}\right)^{n+2} P_n^m(\cos\theta). \tag{24}$$

Thus the condition (11) on the jump in $\mathbf{H}$ at $r = c$, in the uniform conductance case, yields

$$\left.\frac{\partial S_n^{mc}}{\partial r}\right|_{r=c} = -c\left[g_n^m + \frac{\mathscr{G}\mu_0 c}{n} \dot{g}_n^m\right]\left(\frac{a}{c}\right)^{n+2}, \tag{25}$$

$$\left.\frac{\partial S_n^{ms}}{\partial r}\right|_{r=c} = -c\left[h_n^m + \frac{\mathscr{G}\mu_0 c}{n} \dot{h}_n^m\right]\left(\frac{a}{c}\right)^{n+2}, \tag{26}$$

where $\dot{g}_n^m$ and $\dot{h}_n^m$ are the spherical harmonic expansion coefficients of the secular variation. These equations now contain the information required to deduce the horizontal components of the poloidal field and their temporal variation at the CMB from geomagentic field models and secular variation models derived from observations at or above the surface of the Earth.

TEMPORAL EVOLUTION OF $B_{P\theta}$ AND $B_{P\phi}$ AT THE CMB

It is seen that the presence of an infinitesimally thin spherical sheet of non-zero conductance at the base of the mantle gives rise to a jump in the horizontal components of the poloidal magnetic field across the sheet on account of surface currents induced in the sheet due to changes in the magnetic flux threading the sheet, produced by core dynamo processes. Since the poloidal magnetic field components at or above the surface of the Earth are known, the problem is usually inverted in that one seeks to deduce the poloidal field components at the CMB and their temporal variation by downward continuation of the surface fields. This information in turn is used to estimate the fluid flow near the surface of the Earth's outer core, assuming the outer core to be a perfect conductor (Bloxham & Jackson 1991, and references therein). In most of these calculations only the secular variation of the radial component has been used, with the assumption that the mantle is an electrical insulator. However, in order to determine the radial gradient of the flow or the flow shear near the top of the core, it becomes necessary to use the secular variation of the horizontal poloidal components $B_{P\theta}$ and $B_{P\phi}$ (Jackson & Bloxham 1991). Knowledge of $B_{P\phi}$ at the CMB is also required in order to compute the poloidal part, Γ_P, of the electromagnetic

couple which acts on the conducting mantle owing to currents flowing in it (Stix & Roberts 1984; Love & Bloxham 1994):

$$\Gamma_{\rm P} = -\frac{c}{\mu_0}\oint_{\rm CMB} B_{{\rm P}\phi} B_r \sin\theta \, dS . \tag{27}$$

In the present paper, the relatively high conductivity of the lowermost region of the mantle is taken into consideration by modelling it as an infinitesimally thin conducting spherical sheet at the CMB. Continuity of the radial component across the sheet still ensures that results derived from the secular variation of the radial component remain unchanged. However, the horizontal components of the poloidal field $B_{{\rm P}\theta}$ and $B_{{\rm P}\phi}$ at the top of the core are now obtained by using eqs (25) and (26) together with eqs (16) and (19):

$$B_{{\rm P}\theta} = -\sum_{n=1}^{\infty}\sum_{m=0}^{n}[G_n^m \cos m\phi + H_n^m \sin m\phi]\left(\frac{a}{c}\right)^{n+2}\frac{dP_n^m}{d\theta}(\cos\theta), \tag{28}$$

$$B_{{\rm P}\phi} = \frac{1}{\sin\theta}\sum_{n=1}^{\infty}\sum_{m=0}^{n} m[G_n^m \sin m\phi - H_n^m \cos m\phi] \times \left(\frac{a}{c}\right)^{n+2} P_n^m(\cos\theta), \tag{29}$$

where the coefficients G_n^m and H_n^m differ from g_n^m and h_n^m:

$$G_n^m = -\frac{1}{c}\frac{\partial S_n^{mc}}{\partial r}\bigg|_{r=c}\left(\frac{c}{a}\right)^{n+2} = g_n^m + \frac{\mathscr{G}\mu_0 c}{n}\dot{g}_n^m, \tag{30}$$

$$H_n^m = -\frac{1}{c}\frac{\partial S_n^{ms}}{\partial r}\bigg|_{r=c}\left(\frac{c}{a}\right)^{n+2} = h_n^m + \frac{\mathscr{G}\mu_0 c}{n}\dot{h}_n^m . \tag{31}$$

As a consequence of the above, secular variation of the horizontal poloidal components at the top of the core is determined by the time derivatives $\dot{G}_n^m$ and $\dot{H}_n^m$ instead of the usual secular variation coefficients $\dot{g}_n^m$ and $\dot{h}_n^m$:

$$\dot{G}_n^m = \dot{g}_n^m + \frac{\mathscr{G}\mu_0 c}{n}\ddot{g}_n^m, \tag{32}$$

$$\dot{H}_n^m = \dot{h}_n^m + \frac{\mathscr{G}\mu_0 c}{n}\ddot{h}_n^m, \tag{33}$$

where $\ddot{g}_n^m$ and $\ddot{h}_n^m$ are the secular acceleration model coefficients. As can be seen from eqs (30) and (31), the parameter $\tau_m = \mathscr{G}\mu_0 c$ may be defined as an electromagnetic time constant associated wih the mantle. Magnetic field variations on time-scales $\gg\tau_m$ are unaffected by the conductivity of the mantle. The correction terms in eqs (30)–(33) are simply $1/n$-weighted versions of the secular variation/acceleration. The results given in eqs (30) and (31) can be obtained from the results derived by earlier workers (Chapman & Whitehead 1923; Lahiri & Price 1939) if the total internal fields in their formulae are identified wih $\mathbf{B}_{\rm P}(r=c)$.

For the purpose of estimating the effect of a thin layer of high conductivity at the base of the mantle, the effective conductance of the sheet is considered to be 10^8 S (Stewart *et al.* 1995). The choice of this value is discussed later in this section. With the permeability of free space $\mu_0 = 4\pi\times10^{-7}$ H m^{-1} and the core radius $c = 3485$ km, it is seen that $\tau_m \simeq 13.9$ yr. The GSFC(9/80) field model of Langel, Estes & Mead (1982), which provides the main field and secular variation coefficients up to $n=13$ as well as secular acceleration coefficients up to $n=6$ for the 1980 epoch, is used to determine the coefficients G_n^m and H_n^m and their secular variation $\dot{G}_n^m$ and $\dot{H}_n^m$ from eqs (30), (31), (32) and (33).

The coefficients G_n^m and H_n^m, determined using the g_n^m, h_n^m, $\dot{g}_n^m$ and $\dot{h}_n^m$ coefficients of the GSFC(9/80) model up to $n=8$, are utilized to calculate $B_{{\rm P}\theta}$ and $B_{{\rm P}\phi}$ as given by eqs (28) and (29). Figs 1(a) and 2(a) show respectively the contour plots of $B_{{\rm P}\theta}$ and $B_{{\rm P}\phi}$ at the top of the core when the mantle is assumed to be an insulator, while the corrections to $B_{{\rm P}\theta}$ and $B_{{\rm P}\phi}$ due to the presence of the conducting sheet at the base of the mantle are contoured in Figs 1(b) and 2(b). These corrections are seen to by typically $\leq$10 per cent and hence may not be significant. On the other hand, the coefficients $\dot{G}_n^m$ and $\dot{H}_n^m$ up to $n=4$ given in Table 1 differ considerably from $\dot{g}_n^m$ and $\dot{h}_n^m$, so that the corrections to the secular variations in the horizontal components of the poloidal field are typically 40 per cent for an assumed sheet conductance of 10^8 S, as depicted in Figs 3 and 4. It should be noted that the corrections are directly proportional to the conductance $\mathscr{G}$. Terms up to $n=6$ have been used in the computation of the corrections shown in Figs 3 and 4 because secular acceleration coefficients are only available up to $n=6$ in the GSFC(9/80) model. Langel *et al.* (1982) have also listed, in their Tables 4(a) and (b), the standard errors in the estimates of various coefficients for the GSFC(9/80) model, including the first derivatives (secular variation) and second derivatives (secular acceleration). It is seen from these tables that for a majority of the second derivatives of the Gauss coefficients up to $n=6$, the ratio of the coefficient magnitude to the standard error of the coefficient falls in the range 10–25. Considering the upper limit of the standard errors in the secular acceleration coefficients, the corrections to the secular variation in the horizontal components of the poloidal field at the CMB computed in the present paper would still be typically $\geq$30 per cent, for an assumed sheet conductance of 10^8 S.

Changes in the radial flux threading the sheet occur due to a combination of induction resulting from fluid flow near the top of the core and magnetic diffusion. The latter process

Table 1. Secular variation coefficients for $\dot{B}_{{\rm P}\theta}$ and $\dot{B}_{{\rm P}\phi}$ at the top of the core, compared to the secular variation coefficients for $\dot{B}_{m\theta}$ and $\dot{B}_{m\phi}$ at $r=c$ obtained from the GSFC(9/80) magnetic field model for epoch 1980. The coefficients $\dot{G}_n^m$ and $\dot{H}_n^m$ are specified only for the core field at $r=c$, whereas the coefficients $\dot{g}_n^m$ and $\dot{h}_n^m$ are specified for the insulating part of the mantle as well as for $r\geq a$.

n	m	$\dot{G}_n^m$ (nT yr^{-1})	$\dot{g}_n^m$ (nT yr^{-1})	$\dot{H}_n^m$ (nT yr^{-1})	$\dot{h}_n^m$ (nT yr^{-1})
1	0	9.18	20.51		
1	1	2.84	9.08	7.06	−9.04
2	0	−15.44	−19.53		
2	1	8.23	4.78	−38.76	−18.74
2	2	14.68	9.86	−35.26	−26.82
3	0	10.55	4.51		
3	1	2.64	−3.55	−15.85	−5.57
3	2	−0.56	−2.19	0.92	1.64
3	3	9.18	3.87	−8.89	−6.62
4	0	−3.06	−2.20		
4	1	−2.53	−2.24	2.83	3.66
4	2	−12.89	−10.09	1.31	1.08
4	3	−4.74	−3.82	10.62	6.77
4	4	−7.10	−5.54	−3.40	−2.73

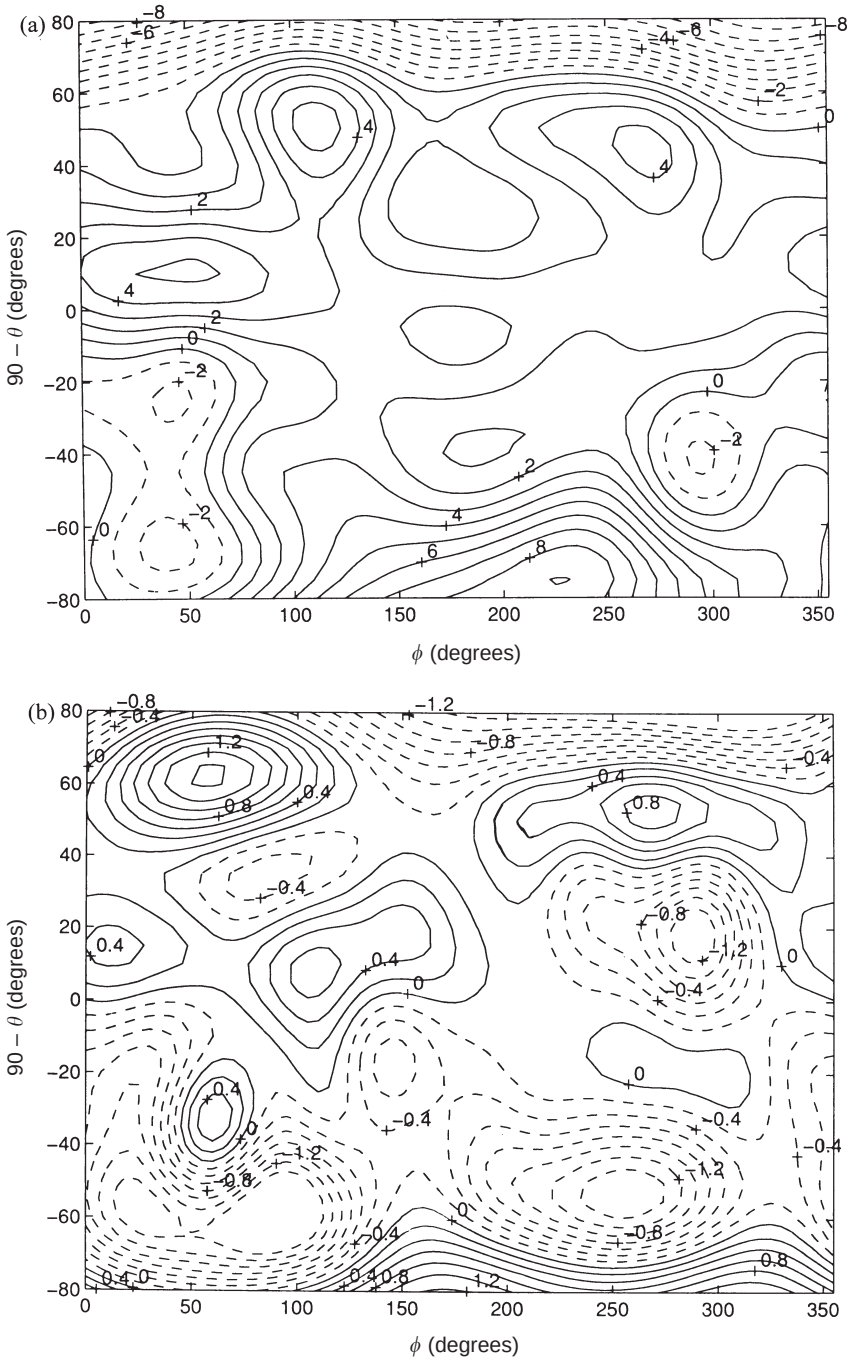

Figure 1. (a) Contour plot of $B_{P\theta}$ at the CMB for epoch 1980, from the GSFC(9/80) model with maximum $n = 8$, assuming a source-free mantle. Contour interval is 10^5 nT. (b) Contour plot of corrections to $B_{P\theta}$ at the CMB for epoch 1980, from the GSFC(9/80) model with maximum $n = 8$, due to the presence of a conducting sheet of conductance 10^8 S at the base of the mantle. Contour levels are marked in units of 10^4 nT and the contour interval is 0.2×10^4 nT.

is important for small-scale features in the magnetic field which would have a diffusion time comparable to the timescale of secular variation. The occurrence of n in the denominators of the correction terms in eqs (32) and (33) leads to the suppression of small-scale features in the corrections to the secular variation of the horizontal components of the poloidal field at the top of the core due to currents induced in the uniformly conducting sheet at the CMB. The signatures of emerging 'core spots' in plots such as Figs 3(b) and 4(b), produced by currents induced in the sheet which tend to flow in circles around regions where there is increasing or decreasing radial magnetic flux, will hence be diffuse in nature.

A conductance of 10^8 S for the lowermost reaches of the mantle may not be entirely implausible. Fig. 5 of Stewart *et al.* (1995) shows the conductance for various radius intervals, starting at the CMB, obtained from 10 published profiles of

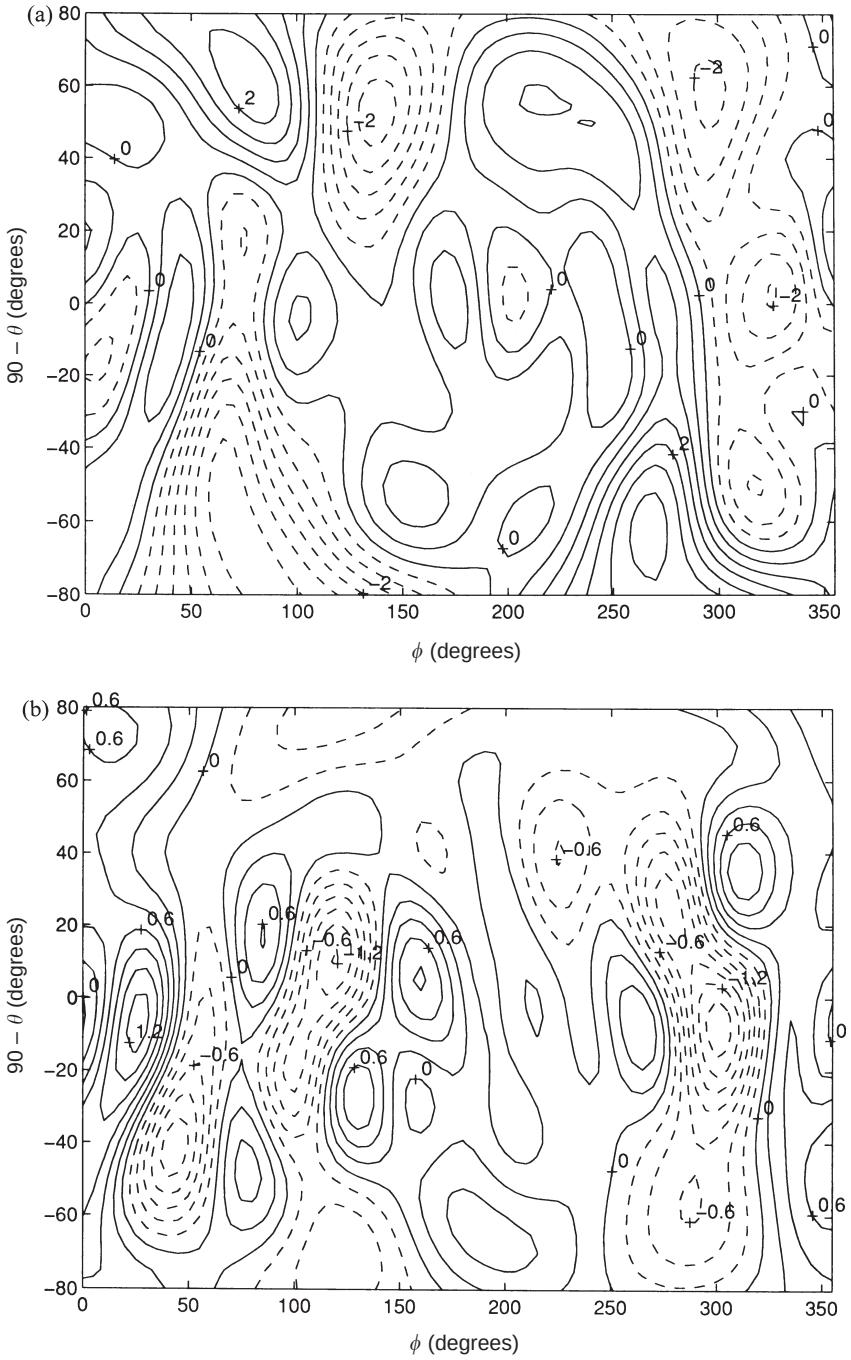

Figure 2. (a) Contour plot of $B_{P\phi}$ at the CMB for epoch 1980, from the GSFC(9/80) model with maximum $n = 8$, assuming a source-free mantle. Contour interval is 0.5×10^5 nT. (b) Contour plot of corrections to $B_{P\phi}$ at the CMB for epoch 1980, from the GSFC(9/80) model with maximum $n = 8$, due to the presence of a conducting sheet of conductance 10^8 S at the base of the mantle. Contour interval is 0.2×10^4 nT.

lower-mantle electrical conductivity. In three of these models, those of Backus (1983), Courtillot & Le Mouël (1984) and Stix & Roberts (1984) respectively, the highly conducting region of the mantle is essentially confined to a thin layer just above the CMB, and the conductance of this layer is $\geq 10^8$ S. In their own study of the electromagnetic torque acting on an electrically conducting mantle, Stewart *et al.* (1995) found a clear correlation, over an 80 year period, between a computed time-varying electromagnetic torque acting on the mantle and the torque acting on the mantle which was inferred from astronomically determined changes in the Earth's rotation period. Their calculation of the electromagnetic torque assumed the mantle to be an electrical insulator except for a thin layer of finite conductance adjacent to the CMB, and their regression analysis yielded a conductance of $(6.7 \pm 0.9) \times 10^8$ S for this layer. This also supports the present assumption regarding the effective conductance of the lowermost mantle and the thin-sheet approximation used here.

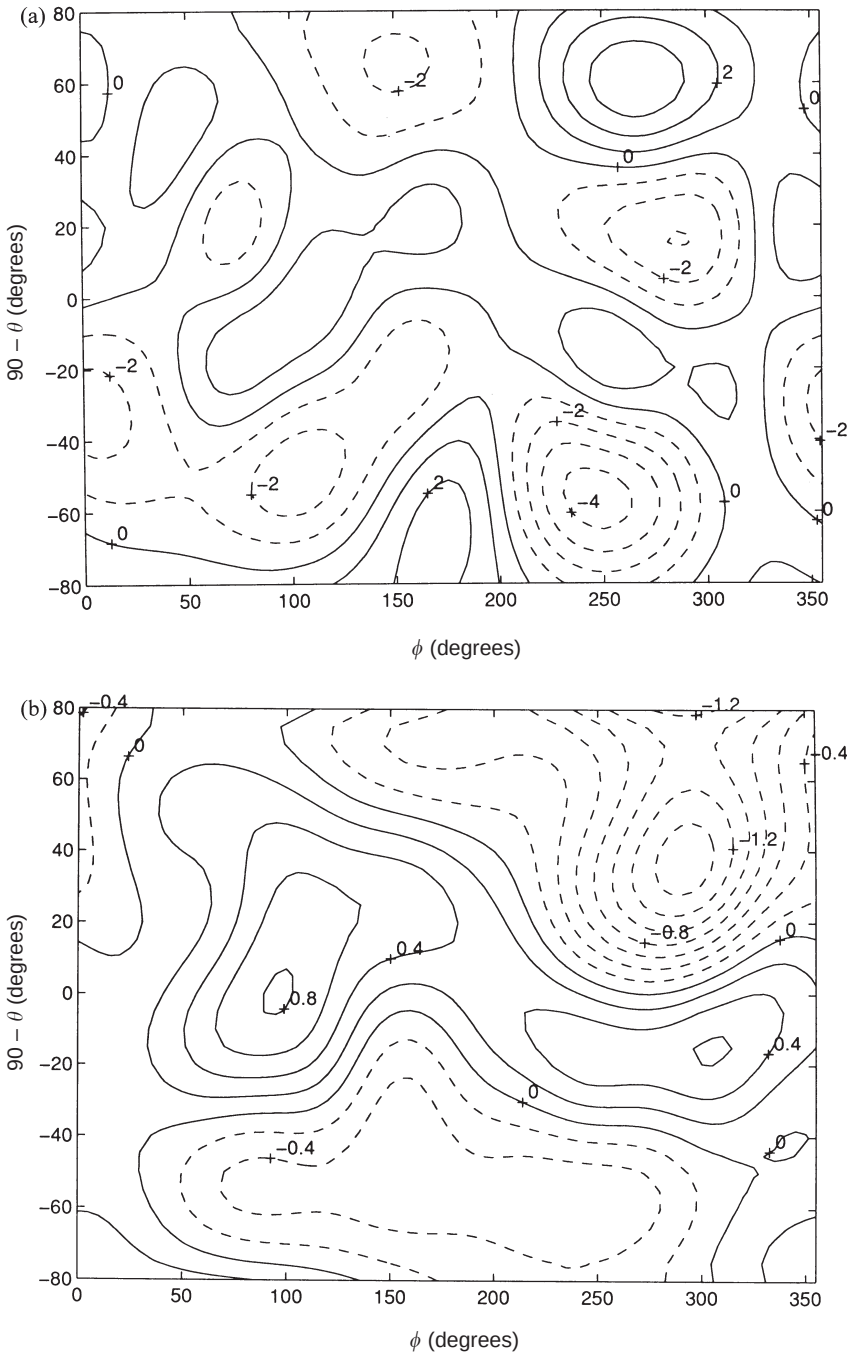

Figure 3. (a) Contour plot of $\dot{B}_{P\theta}$ at the CMB for epoch 1980, from the GSFC(9/80) model with maximum $n = 6$, assuming a source-free mantle. Contour interval is 10^3 nT/yr. (b) Contour plot of corrections to $\dot{B}_{P\theta}$ at the CMB for epoch 1980 from the GSFC(9/80) model with maximum $n = 6$, due to the presence of a conducting sheet of conductance 10^8 S at the base of the mantle. Contour levels are marked in units of 10^3 nT yr^{-1} and the contour interval is 0.2×10^3 nT yr^{-1}.

COMPARISON WITH PERTURBATION SOLUTION

A perturbation procedure was developed by Benton & Whaler (1983) to obtain a solution to the inverse poloidal diffusion problem in a weakly conducting mantle, with a radially symmetric distribution of conductivity. In their work, the poloidal magnetic field in the conducting mantle was given in terms of the poloidal function S:

$$\mathbf{B}_P = \nabla \times \nabla \times (r S \hat{\mathbf{r}}), \tag{34}$$

with

$$S = a \sum_{n=1}^{\infty} \sum_{m=0}^{n} [\alpha_n^m(r, t) \cos m\phi + \beta_n^m(r, t) \sin m\phi] P_n^m(\cos\theta). \tag{35}$$

The α_n^m, β_n^m were obtained as series solutions of the form

$$n\alpha_n^m(r, t) = f_{0n}^m(r) g_n^m(t) + f_{1n}^m(r) \dot{g}_n^m(t) + f_{2n}^m(r) \ddot{g}_n^m(t) + \ldots, \tag{36}$$

where, omitting the sub- and superscripts n and m as in the

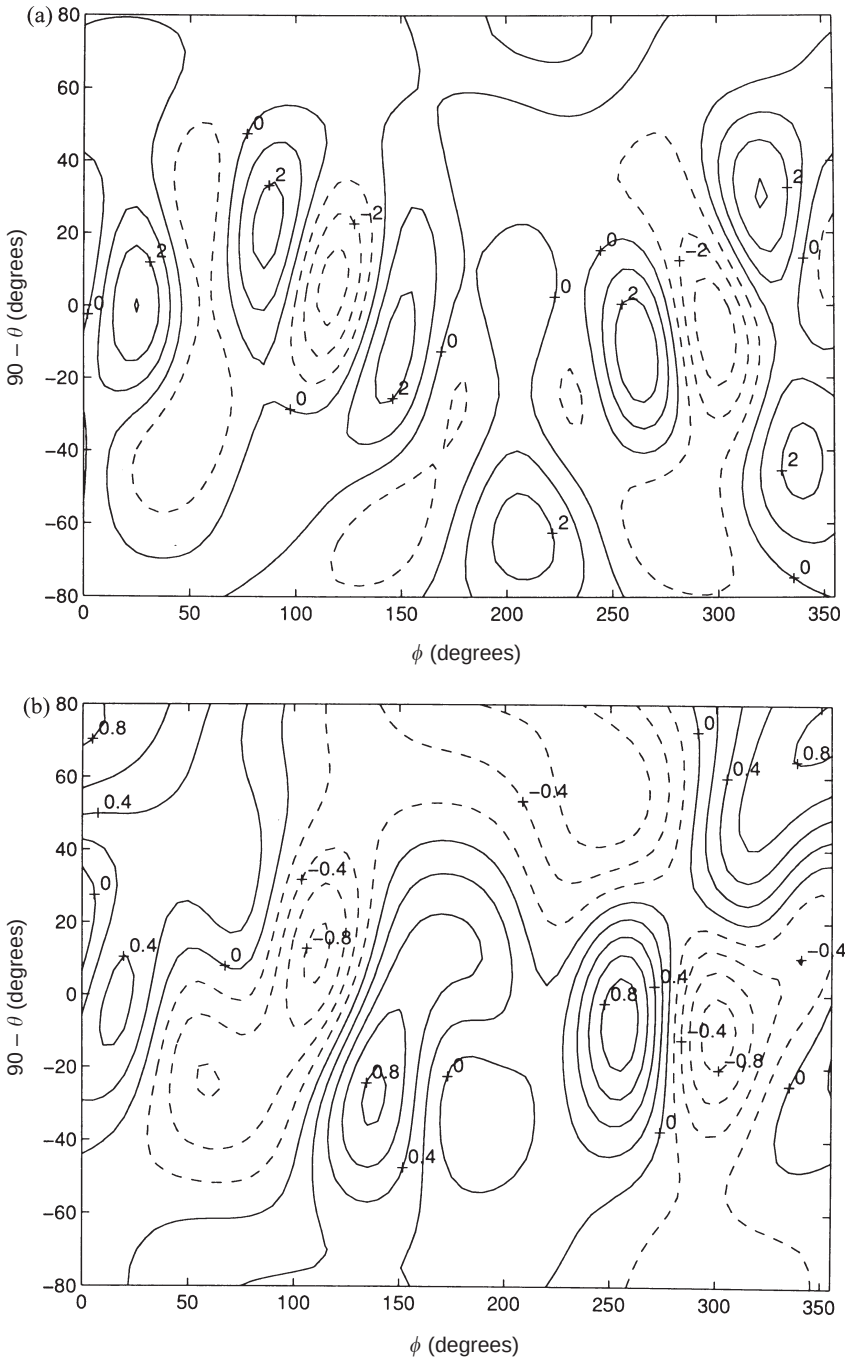

Figure 4. (a) Contour plot of $\dot{B}_{P\phi}$ at the CMB for epoch 1980, from the GSFC(9/80) model with maximum $n = 6$, assuming a source-free mantle. Contour interval is 10^3 nT yr^{-1}. (b) Contour plot of corrections to $\dot{B}_{P\phi}$ at the CMB for epoch 1980, from the GSFC(9/80) model with maximum $n = 6$, due to the presence of a conducting sheet of conductance 10^8 S at the base of the mantle. Contour interval is 0.2×10^3 nT yr^{-1}.

work of Benton & Whaler (1983), the functions $f_i(r)$ were given by

$$f_0(r) = \left(\frac{a}{r}\right)^{n+1}, \tag{37}$$

$$f_i(r) = \frac{a\mu_0}{2n+1}\left(\frac{a}{r}\right)^{n+1}\int_r^a \left[1 - \left(\frac{r}{\xi}\right)^{2n+1}\right]\left(\frac{\xi}{a}\right)^{n+2} \times \sigma(\xi) f_{i-1}(\xi)\, d\xi, \qquad i = 1, 2, 3, \ldots. \tag{38}$$

Continuity of B_r at the CMB implies that at $r = c$, the $S_n^m(r, t)$ defined in eq. (19) is given by

$$S_n^{mc}(c, t) = ac\alpha_n^m(c, t). \tag{39}$$

For a mantle of finite conductivity and thickness, continuity of j_r, B_θ and B_ϕ at the CMB implies that

$$\left.\frac{\partial S_n^{mc}}{\partial r}\right|_{r=c} = a\alpha_n^m(c, t) + ac\left.\frac{\partial \alpha_n^m}{\partial r}\right|_{r=c}. \tag{40}$$

For a mantle conductivity distribution where $\sigma(r)$ is non-zero only in a thin shell of thickness $\delta \ll c$ adjacent to the CMB, even if σ is very large and the conductance $\mathscr{G}$ is defined by eq. (6), an expansion in terms of δ/c yields the following zeroth-order results:

$$f_1(c) = 0, \tag{41}$$

$$\left.\frac{\partial f_1}{\partial r}\right|_{r=c} = -\mu_0 \mathscr{G} \left(\frac{a}{c}\right)^{n+1}, \tag{42}$$

$$f_i(c) = 0 \qquad \text{for } i > 1, \tag{43}$$

$$\left.\frac{\partial f_i}{\partial r}\right|_{r=c} = 0 \qquad \text{for } i > 1. \tag{44}$$

Thus for a conducting layer of finite thickness $\delta \ll c$ at the base of the mantle, eqs (39) and (40) lead to zeroth-order expressions in tems of δ/c which are identical to eqs (20) and (25). For $S_n^{ms}(c, t)$ and the radial derivative of $S_n^{ms}(r, t)$ at $r = c$, zeroth-order expressions are likewise obtained which are identical to eqs (21) and (26).

In their evaluation of the time-dependent poloidal couple, parallel to the Earth's rotation axis, which acts on the mantle owing to its electromagnetic coupling with the core, Stix & Roberts (1984) solved the induction equation in the mantle by iteration (Benton & Whaler 1983) for the case where the mantle conductivity was confined to a layer of thickness $(b - c)$, adjacent to the CMB:

$$\sigma(r) = \sigma_c (r/c)^{-\alpha}, \qquad c < r < b. \tag{45}$$

With $b = c + \delta$, it is seen that in the limit $\sigma_c \to \infty$ and $\delta \to 0$ such that $\sigma_c \delta$ is finite, the conductance $\mathscr{G} = \sigma_c \delta$. In this limit, eq. (41) for the poloidal couple, derived by Stix & Roberts (1984), reduces to

$$\Gamma_P = 4\pi c^4 \mathscr{G} \sum_{n=1}^{\infty} \sum_{m=0}^{n} \frac{m(n+1)}{n(2n+1)} \left(\frac{a}{c}\right)^{2n+4} (g_n^m \dot{h}_n^m - h_n^m \dot{g}_n^m), \tag{46}$$

which is precisely the result that would be obtained by substituting eq. (29) for $B_{P\phi}(r = c)$ in eq. (27). In Fig. 5, Γ_P is plotted for the period 1840–1990 using the time-dependent field model of Bloxham & Jackson (1992) and for two values of the conductance, $\mathscr{G} = 5 \times 10^7$ S and $\mathscr{G} = 10^8$ S. As in Fig. 1 of Stix & Roberts (1984), the time variation of Γ_P is more pronounced for the higher conductance. For the three cases considered by those authors, the conductance of the mantle was 1.3×10^8 S, 2.4×10^8 S and 3.5×10^8 S respectively, while the thickness of the conducting layer was 2000 km in each case. The results obtained in this section show that perturbation solutions derived for a layer of finite thickness converge to the exact results derived here in the limit of an infinitesimally thin layer of finite conductance.

CONCLUSIONS

There is a general awareness among geophysicists working in this area of the effect that an electrically conducting layer at the base of the mantle might have on the downward continuation of the poloidal geomagnetic field to the CMB. Quantitative estimates of this effect have been based on an iterative solution of the induction equation in the mantle involving a low-conductivity expansion (Roberts 1972; Backus 1982; Benton & Whaler 1983). The exercise undertaken in the present paper is not restricted to a weakly conducting mantle and thus offers a general method for the determination of the horizontal components of the poloidal field and their temporal evolution at the top of the core in the presence of a highly conducting sheet adjacent to the CMB. In fact, it also demonstrates that the perturbation results need not be restricted to low conductivity when the conductivity in the mantle is confined to a very thin shell at the base of the mantle.

Both the radial and the horizontal components of the induction equation, which governs the temporal evolution of the magnetic field produced by the geodynamo, were used, for

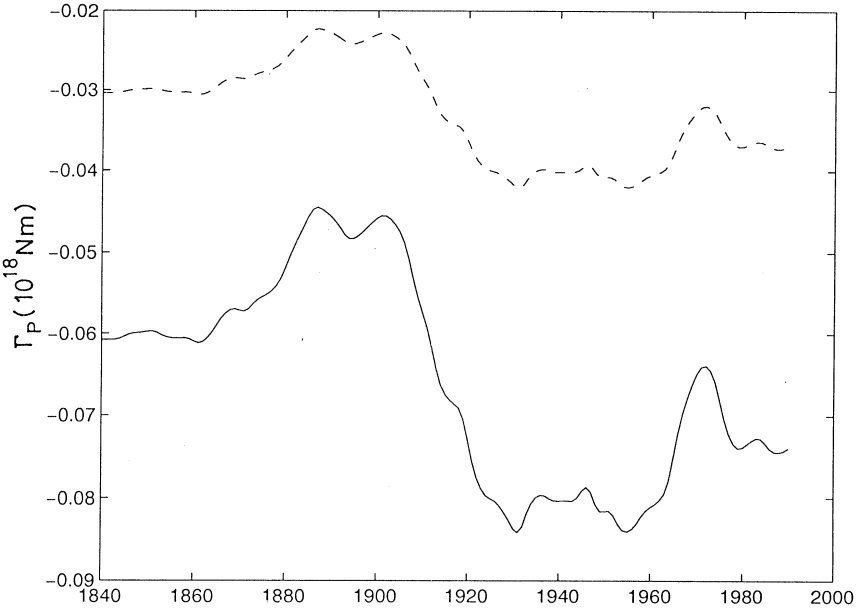

Figure 5. The poloidal torque, Γ_P, as a function of time for two effective conductances of the conducting sheet at the base of the mantle. The solid line is for $\mathscr{G} = 10^8$ S and the dashed line is for $\mathscr{G} = 5 \times 10^7$ S.

the first time, by Lloyd & Gubbins (1990) to estimate a toroidal flow and shear at the top of the core. This was followed by the determination of a general steady flow and shear, a steady geostrophic flow and shear, and a steady toroidal flow and shear for the interval 1960–1980 by Jackson & Bloxham (1991). In the latter work, the authors found that the shear tends to be either parallel or antiparallel to the flow, such that the flow weakens or strengthens with depth near the top of the core. It may be of interest to note that the surface helicity density would be nearly zero in a situation in which the flow shear tends to be either parallel or antiparallel to the flow. Thus any substantial change in the direction of flow shear in such a situation, brought about by corrections to the secular variation of the horizontal components of the poloidal field at the top of the core, would bring about a considerable change in the estimated surface helicity density. Since the ratio of flow to shear gives an idea of the vertical scale length associated with a convection cell (Bloxham & Jackson 1991), some of these ideas regarding the flow pattern derived from earlier estimates of shear, as also the pattern of lateral temperature variations just beneath the CMB deduced from the thermal wind equation which governs geostrophic motion of the fluid near the CMB (Bloxham & Jackson 1990), may stand altered if the secular variation of the horizontal components of the poloidal field is corrected for non-vanishing mantle conductivity.

A major drawback of the present calculation is the assumption of a uniform conductance for the sheet, which is not realistic. In future work, lateral variations in the conductivity of the most highly conducting region at the base of the mantle must be considered. With the improved accuracy of geomagnetic field models and secular variation models expected from the planned Ørsted Geomagnetic Research Satellite Mission, such calculations might not be meaningless. Treatment of heterogeneities in the mantle conductivity near the CMB may become more tractable with the thin-sheet approximation used in the present study. However, consideration of lateral inhomogeneities in the conductivity introduces another unknown, the toroidal scalar T in eq. (11). In that situation, condition (11) serves to couple the poloidal and toroidal components of the magnetic field, as considered by Busse & Wicht (1992), who have explored the possibility of a simple dynamo caused by conductivity variations in a planar model, and concluded that lateral variations of electrical conductivity in the lower mantle may have a significant influence on the geodynamo.

REFERENCES

Backus, G.E., 1982. The electric field produced in the mantle by the dynamo in the core, *Phys. Earth planet. Inter.,* **28,** 191–214.

Backus, G.E., 1983. Application of mantle filter theory to the magnetic jerk of 1969, *Geophys. J. R. astr. Soc.,* **74,** 713–746.

Barraclough, D.R., Gubbins, D. & Kerridge, D., 1989. On the use of horizontal components of magnetic field in determining core motions, *Geophys. J. Int.,* **98,** 293–299.

Benton, E.R. & Whaler, K.A., 1983. Rapid diffusion of the poloidal magnetic field through the weakly conducting mantle: A perturbation solution, *Geophys. J. R. astr. Soc.,* **75,** 77–100.

Bloxham, J. & Jackson, A., 1990. Lateral temperature variations at the core–mantle boundary deduced from the magnetic field, *Geophys. Res. Lett.,* **17,** 1997–2000.

Bloxham, J. & Jackson, A., 1991. Fluid flow near the surface of Earth's outer core, *Rev. Geophys.,* **29,** 97–120.

Bloxham, J. & Jackson, A., 1992. Time dependent mapping of the magnetic field at the core–mantle boundary, *J. Geophys. Res.,* **97,** 19 537–19 563.

Busse, F.H. & Wicht, J., 1992. A simple dynamo caused by conductivity variations, *Geophys. astrophys. Fluid Dyn.,* **64,** 135–144.

Chapman, S. & Whitehead, T.T., 1923. The influence of electrically conducting material within the earth on various phenomena of terrestrial magnetism, *Trans. Camb. phil. Soc.,* **22,** 463–482.

Courtillot, V. & Le Mouël, J.L., 1984. On Backus, mantle filter theory and the 1969 geomagnetic impulse, *Geophys. J. R. astr. Soc.,* **78,** 619–625.

Jackson, A. & Bloxham, J., 1991. Mapping the fluid flow and shear near the core surface using the radial and horizontal components of the magnetic field, *Geophys. J. Int.,* **105,** 199–212.

Knittle, E. & Jeanloz, R., 1989. Simulating the core mantle boundary: an experimental study of high pressure reactions between silicates and liquid iron, *Geophys. Res. Lett.,* **7,** 609–612.

Knittle, E. & Jeanloz, R., 1991. Earth's core–mantle boundary: Results of experiments at high pressures and high temperatures, *Science,* **251,** 1438–1443.

Lahiri, B.N. & Price, A.T., 1939. Electromagnetic induction in non-uniform conductors and the determination of the conductivity of the Earth from terrestrial magnetic variation, *Phil. Trans. R. Soc. Lond.,* A, **237,** 509–540.

Langel, R.A., Estes, R.H. & Mead, G.D., 1982. Some new methods in geomagnetic field modelling applied to the 1960–80 epoch, *J. Geomag. Geoelectr.,* **34,** 327–349.

Lloyd, D. & Gubbins, D., 1990. Toroidal fluid motion at the top of Earth's core, *Geophys. J. Int.,* **100,** 455–467.

Love, J.J. & Bloxham, J., 1994. Electromagnetic coupling and the toroidal magnetic field at the core–mantle boundary, *Geophys. J. Int.,* **117,** 235–256.

Parkinson, W.D. & Hutton, V.R.S., 1989. The electrical conductivity of the Earth, in *Geomagnetism,* Vol. 3, pp. 261–321, ed. Jacobs, J.A., Academic Press, London.

Poirier, J.P. & Le Mouël, J.L., 1992. Does infiltration of core material into the lower mantle affect the observed geomagnetic field? *Phys. Earth planet. Inter.,* **73,** 29–37.

Rikitake, T., 1966. *Electromagnetism and the Earth's Interior,* Elsevier, Amsterdam.

Roberts, P.H., 1972. Electromagnetic core–mantle coupling, *J. Geomag. Geoelectr.,* **24,** 231–259.

Stacey, F.D., 1992. *Physics of the Earth,* Brookfield, Brisbane.

Stewart, D.N., Busse, F.H., Whaler, K.A. & Gubbins, D., 1995. Geomagnetism, Earth rotation and the electrical conductivity of the lower mantle, *Phys. Earth planet. Inter.,* **92,** 199–214.

Stix, M. & Roberts, P.H., 1984. Time-dependent electromagnetic core–mantle coupling, *Phys. Earth planet. Inter.,* **36,** 49–60.